

Controlling the Fiber Diameter during Electrospinning

Sergey V. Fridrikh,¹ Jian H. Yu,¹ Michael P. Brenner,² and Gregory C. Rutledge^{1,*}

¹*Department of Chemical Engineering, Massachusetts Institute of Technology,
77 Massachusetts Avenue, Cambridge, Massachusetts 02139*

²*Division of Engineering and Applied Sciences, Harvard University, 29 Oxford Street, Cambridge, Massachusetts 02138*
(Received 1 November 2002; published 8 April 2003)

We present a simple analytical model for the forces that determine jet diameter during electrospinning as a function of surface tension, flow rate, and electric current in the jet. The model predicts the existence of a terminal jet diameter, beyond which further thinning of the jet due to growth of the whipping instability does not occur. Experimental data for various electrospun fibers attest to the accuracy of the model.

DOI: 10.1103/PhysRevLett.90.144502

PACS numbers: 47.20.-k, 47.65.+a, 47.85.-g, 81.05.Lg

Electrostatic fiber formation, or “electrospinning,” is a method of producing fibers with diameters ranging from 10 μm to 10 nm by accelerating a jet of charged polymer solution in an electric field. The technology has attracted much attention recently [1–9] due to the ease with which nanometer diameter fibers can be produced from either natural [1] or synthetic [2] polymers. Such small fibers have numerous and diverse potential applications including filtration [3] and composite materials [4,5]. Their high surface area makes nanofibers attractive as catalyst supports [6], and in drug delivery [7]. Electrospun nonwoven fabrics are being developed for tissue engineering [8]. Electrospun conducting polymers have been used to fabricate nanowires [9].

Control over the fiber diameter remains a technological bottleneck. Empirical observations indicate that the smallest diameters occur at the lowest flow rates, where production rates are lowest. Since most electrospun fibers are produced from solution, the dry fiber diameter can also vary with the solution concentration [10], due to removal of solvent; however, this approach to control the diameter is limited to the narrow window of spinnable solution concentration.

In this paper, we present a simple model for the stretching of a viscous charged fluid in an electric field. This model suggests that there is a limiting diameter for the fluid jet attained during electrospinning. The model predicts that the final diameter of the fluid jet arises from a force balance between surface tension and electrostatic charge repulsion. The predictions quantitatively agree with electrospun fibers produced from solutions of different polymers at various concentrations.

During electrospinning, a reservoir of polymer fluid is contacted with a large electric potential and delivered to the tip of a small capillary. The electrical charge that develops at the fluid’s free surface interacts with the external electric field, resulting in the emission of a steady fluid jet that thins as it accelerates downfield (Fig. 1). In most operations of interest, the jet experiences a whipping instability, leading to bending and stretching of the jet, observed as loops of increasing size as the

instability grows. The whipping jet thins dramatically, by as much as 3 orders of magnitude, while traveling the short distance between the electrodes (up to ~ 30 cm). The presence of polymer in solution leads to the formation of fine solid fibers as the solvent evaporates [11].

Our model of the whipping jet treats the jet as a slender viscous object. The equations describing the motion of the whipping jet were derived previously in [12,13], where they were successfully applied to the linear instability analysis of electrodriven jets, relevant only in the early stages of whipping. To determine how thin the jet can ultimately become, we reexamine these equations for the regime of nonlinear instability. The model solves the equations of motion for the jet, as a function of material properties [conductivity (K), dielectric permittivity (ϵ), dynamic viscosity (μ), surface tension (γ), and density (ρ)] as well as operating characteristics [flow rate (Q), applied electric field (E_∞), and electric current (I)]. In experiments, the current is determined uniquely by fluid,

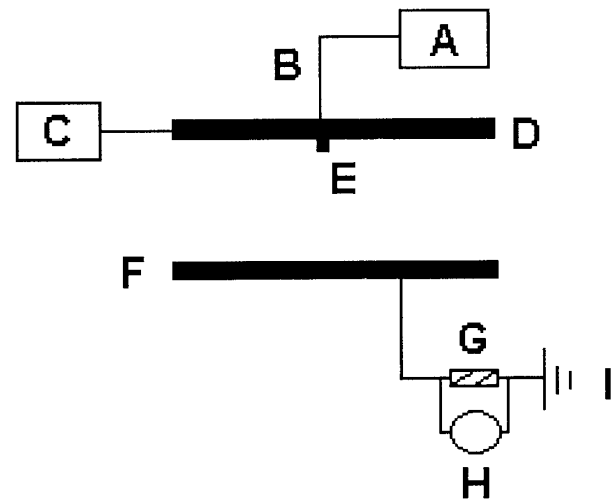


FIG. 1. Schematic representation of the parallel-disk fiber spinner: (a) pump; (b) feed line; (c) voltage supply; (d) upper disk; (e) capillary; (f) lower disk with insulated stand; (g) resistor; (h) voltage meter; (i) ground.

equipment, and operating conditions. The model assumes the fluid is Newtonian and neglects elastic effects due to drying of the jet. The outside medium has dielectric constant $\bar{\epsilon}$, and provides only a uniform external pressure. The jet is characterized by the jet diameter h and radius of curvature R .

Previous analysis of the thinning rate for jets accelerated by tangential electric fields [12] shows that the characteristic length scale of the thinning is the contour length of the jet L , which is typically much larger than the radius of curvature R of whipping. This suggests that the tangential forces can be neglected; mass conservation then implies that the jet thinning arises from the whipping instability itself. The equation of motion for normal displacements x of the centerline of the jet can then be derived from the force and angular momentum balance; see Eqs. (81)–(85) of Ref. [12]. This equation is general and describes both early (linear) and late (nonlinear) stages of whipping. For $h/R \ll 1$ (which is generally the case observed in the lab) and $h/L \ll 1$, terms of higher order in h/R and h/L , involving derivatives with respect to s , can be discarded. The equation of motion of the jet is then

$$\begin{aligned} \rho \pi h^2 \ddot{x} = & 2\pi h \sigma_0 E_\infty \cdot \hat{\xi} \\ & + \left(\pi \gamma + \frac{h \bar{\epsilon}}{2} \beta (E_\infty \cdot \hat{t})^2 \right. \\ & \left. + \frac{2\pi^2 h \sigma_0^2}{\bar{\epsilon}} (3 - 2 \ln \chi) \right) \frac{h}{R}, \end{aligned} \quad (1)$$

where \hat{t} and $\hat{\xi}$ are the unit vectors tangential and normal to the centerline of the jet, $\beta = (\epsilon/\bar{\epsilon} - 1)$. The parameter $\chi \sim R/h$ is the dimensionless wavelength of the instability responsible for the normal displacements.

The first term on the right hand side of Eq. (1) originates from the external electric field acting on the jet's surface charge. The second term is the normal stress due to bending, which gives rise to the whipping instability. If this quantity is negative, the jet is unstable and the whipping instability grows. The first two terms composing this coefficient are surface tension and the tension resisting the bending of electric field lines in the jet. Both of these effects are stabilizing. For very small diameter jets, the surface tension contribution is the more important of the two. The third term is due to surface charge repulsion and is destabilizing. To a first approximation, the stability of the jet to whipping may be viewed as a competition between surface tension and surface charge repulsion:

$$\pi \gamma \geq 2\pi^2 h(z) \sigma_0(z)^2 (2 \ln \chi - 3) / \bar{\epsilon}. \quad (2)$$

When surface tension dominates, inequality (2) is satisfied, and the centerline is straight; when charge repulsion dominates, the perturbations to the centerline grow, and the jet becomes bent. Charge conservation implies that the current is constant and is composed of both conduction and surface charge advection contributions: $I = 2\pi \sigma_0 h v + \pi E K h^2$ (where v is the jet velocity) [13].

The surface charge density near the nozzle is thought to be low [13]. Bulk current dominates advection current here, and the jet is stable. As the jet thins away from the nozzle, the resistance to bulk current increases and advection current becomes important. The surface charge density grows until charge repulsion overcomes surface tension and the jet begins to whip.

When the jet is significantly bent, volume conservation implies that $Q = \pi h^2 v_z (ds/dz)$ where ds/dz is the centerline length of jet (ds) contained in a horizontal slice of thickness dz between the two electrodes, and $v_z(z)$ is the vertical velocity of the loops moving downward. The total current I directed toward the lower electrode is $I = 2\pi \sigma_0 (ds/dz) h v_z + \pi E_t K h^2$, where E_t is now the tangential component of the applied electric field. Combining these two relations, we find $I = 2\sigma_0 Q/h + \pi E_t K h^2$ also in the nonlinear regime. Ultimately, the bulk current is dominated by the advection current, so that $\sigma_0 = Ih/(2Q)$. This implies that, at the late stages of whipping, the right hand side of inequality (2) decreases as h^3 until it exactly balances the surface tension. At this point, the dramatic stretching of the jet due to the whipping instability ceases, and the terminal diameter of the jet is reached.

Substituting $\sigma_0 = hI/2Q$ into Eq. (2), we obtain the relation for the terminal jet radius h_t :

$$h_t = \left(\gamma \bar{\epsilon} \frac{Q^2}{I^2} \frac{2}{\pi(2 \ln \chi - 3)} \right)^{1/3}. \quad (3)$$

Equation (3) predicts that the terminal diameter of the whipping jet is controlled by the flow rate, electric current, and the surface tension of the fluid. Equation (3) neglects elastic effects and fluid evaporation, and also assumes minimal jet thinning after the saturation of the whipping instability. These assumptions are tested by measuring the diameters of electrospun fibers obtained over a wide range of external conditions.

Solutions of polycaprolactone (PCL) exhibit a nonlinear relationship between flow rate and current for flow rates less than 1.0 ml/min. Figure 2 shows a tenfold change in I/Q for flow rates over this range [14]. Hence, Eq. (3) suggests that varying the flow rate Q will yield a $10^{2/3}$ (~ 6) fold variation in fiber diameter.

In Fig. 3 the average diameter of PCL fibers is plotted against Q/I (the inverse of volume charge density). Data for solutions ranging from 8 to 12 wt% PCL are shown. Significantly, variations in diameter of fivefold to sixfold (for 11 and 12 wt% PCL solutions, respectively) have been achieved solely through changing Q/I . Linear regression results in slopes ranging from 0.627 to 0.743, with regression coefficients of 0.899 to 0.998; see Table I for details. Assuming that solvent evaporation is insignificant prior to the attainment of the limiting jet diameter, and that evaporation changes the diameter but not length of the thread, we can estimate the fluid jet diameter which gives rise to a solid fiber by correcting for

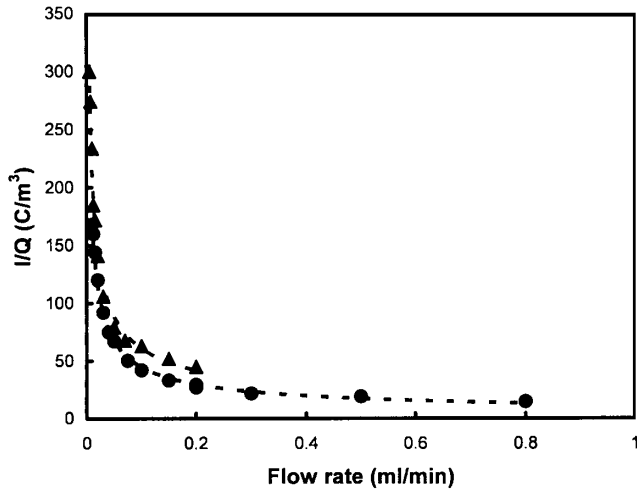


FIG. 2. Relation between the volume charge density (I/Q) and flow rate Q for two solutions of PCL, 11% (\blacktriangle) and 12% (\bullet) by weight, respectively.

polymer concentration, c : $h_t = d/c^{1/2}$. The data for terminal jet diameter as a function of Q/I collapses onto a single line with slope 0.639, in good agreement with the value of $2/3$ predicted by Eq. (3) (see inset of Fig. 3).

Using the known values for surface tension, permittivity, flow rate, and current, as well as an estimate for χ [15], Eq. (3) also predicts the magnitude of h_t and, after correcting for solvent evaporation, the solid fiber diameter. This theoretical curve (inset of Fig. 3) for h_t is shifted below the experimental data by roughly a constant factor of ~ 2 . Remarkably, this level of agreement is obtained with a relatively simple theory and no fitting parameters.

The PCL solutions used here have relatively low conductivity ($< 1 \mu\text{S}/\text{cm}$). We also tested this model using more conductive solutions of polyethylene oxide (PEO) and polyacrylonitrile (PAN). We had less success in electrospinning PEO and PAN solutions over a wide enough range of Q/I to test the $2/3$ scaling definitively. Nevertheless, for flow rates around 0.005 ml/min, the model predicts the fiber diameter of PEO with a remarkable accuracy of about 10% (Fig. 4). For PAN spun at 0.03 ml/min, the model predicts the fiber diameter with

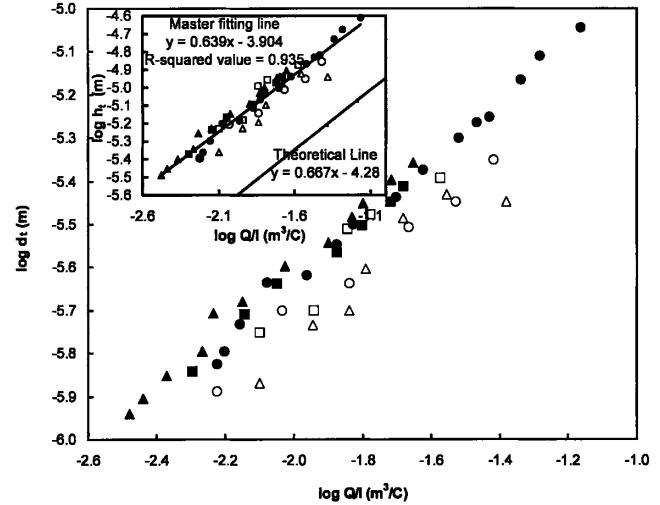


FIG. 3. The log of fiber diameter versus the log of $(I/Q)^{-1}$. The concentrations of PCL shown are 12% (\bullet), 11% (\blacktriangle), 10% (\blacksquare), 9% (\circ), 8.5% (\triangle), and 8% (\square) by weight. The inset shows the terminal jet diameter, d_t as a function of $(I/Q)^{-1}$ compared to the theory.

an error of about 20%. Figure 4 compares the experimental data for fiber diameters and the theoretical values predicted by Eq. (3) for several polymers, solution concentrations, and processing conditions.

The fact that the theory overpredicts stretching for PCL solution and shows such good agreement for PEO and PAN may be due to the difference in charge carriers and solvents. For PEO and PAN the main charge carrier is the polymer itself, and the solvents (water and N,N -dimethyl formamide) are not very volatile. Thus most of the charges stay with the jet until it reaches the collector, and the drying takes place after the stretching. PCL is nonconducting, and the charges are carried by methanol, which is very volatile. In this case, charges carried by evaporated solvent molecules may still reach the collector and contribute to the measured current, I , but not the terminal force balance. This would lead to overprediction of surface charge and underprediction of terminal jet diameter, as seen in Fig. 3. Equation (3) thus

TABLE I. Linear regressions to experimental data for the terminal jet diameter of PCL solutions. The slope predicted by the model is $2/3$. The terminal jet diameter is obtained from the dry fiber data using a correction for polymer concentration (see text for details).

Concentration of PCL	Dry fiber diameter range (μm)	Terminal jet diameter range (μm)	Linear regression slope	Linear regression intercept	Theoretical intercept
12% wt	1.50–6.65	4.07–18.04	0.706	–3.79	–4.29
11% wt	1.15–4.40	3.25–12.46	0.692	–3.75	–4.29
10% wt	1.44–3.87	4.27–11.50	0.659	–3.84	–4.29
9% wt	1.29–4.47	4.15–13.98	0.627	–3.97	–4.28
8.5% wt	1.35–3.57	4.35–11.48	0.650	–3.96	–4.28
8% wt	1.77–4.04	5.87–13.40	0.743	–3.67	–4.27

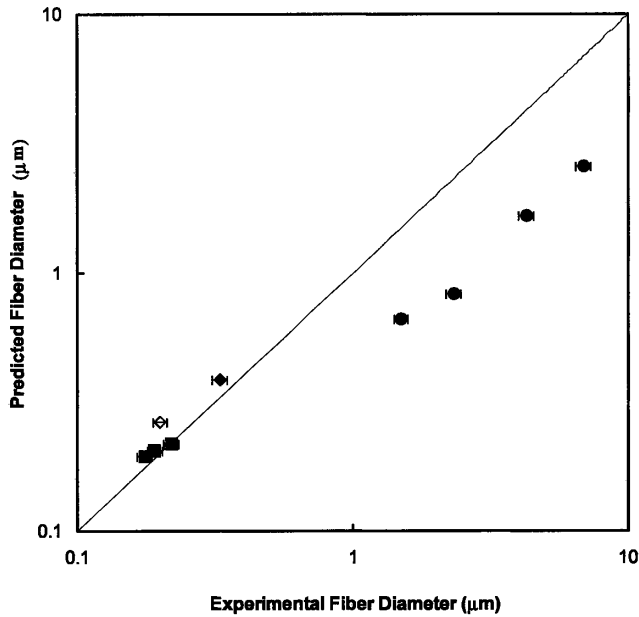


FIG. 4. A comparison of the experimental and predicted fiber diameters: polymer solutions shown are 12% wt PCL (●), 10% wt PAN (◆), 8% wt PAN (◇), and 2% wt PEO (■) at various flow rates and electric currents.

provides an accurate lower bound estimate for the diameter of electrodriven jet.

In summary, we have presented a model of a charged fluid jet in an electric field under conditions applicable to the whipping instability. The model predicts a terminal jet diameter, which is a consequence of balance between normal stresses due to surface tension and surface charge repulsion and can be determined from knowledge of the flow rate, electric current, and the surface tension of the fluid. The $2/3$ scaling with the inverse volume charge density $(I/Q)^{-1}$ predicted by the model is confirmed experimentally using several concentrations of PCL, providing convincing evidence for the correctness of the model. Further support for the model is provided by the reasonable prediction of the dry fiber diameter for PCL, PEO, and PAN.

Financial support for this work was provided by National Textile Centre under Grant No. M01-D22. M. P. B. acknowledges support from the NSF Division of Mathematical Sciences. We thank D. Blankschtein and A. Goldsipe for the help with surface tension measurements.

*Email address: rutledge@mit.edu

[1] M. M. Demir, L. Yilgor, E. Yilgor, and B. Erman, *Polymer* **43**, 3303 (2002); I. D. Norris, M. M. Shaker,

F. K. Ko, and A. G. MacDiarmid, *Synth. Met.* **114**, 109 (2000).

- [2] J. A. Matthews, G. E. Wnek, D. G. Simpson, and G. L. Bowlin, *Biomacromolecules* **3**, 232 (2002); H.-J. Jin, S. V. Fridrikh, G. C. Rutledge, and D. L. Kaplan, *Biomacromolecules* **3**, 1233 (2002).
- [3] P. P. Tsai, H. Schreuder-Gibson, and P. Gibson, *J. Electroanal. Chem.* **54**, 333 (2002).
- [4] J. S. Kim and D. H. Reneker, *Polym. Compos.* **20**, 124 (1999).
- [5] A. Ali *et al.*, in *Proceedings of TEXCOMP-6, International Conference on Textile Composites, Philadelphia, PA, 2002* (available as CD-ROM from the organizers of TEXCOMP-6).
- [6] H. Jia *et al.*, *Biotechnol. Prog.* **18**, 1027 (2002).
- [7] E. R. Kenawy *et al.*, *J. Controlled Release* **81**, 57 (2002).
- [8] W. Li *et al.*, *J. Biomed. Mater. Res.* **60**, 613 (2002).
- [9] A. G. MacDiarmid *et al.*, *Synth. Met.* **119**, 27 (2001).
- [10] J. M. Deitzel, J. Kleinmeyer, D. Harris, and N. C. B. Tan, *Polymer* **42**, 261 (2001).
- [11] M. Shin, M. M. Hohman, M. P. Brenner, and G. C. Rutledge, *Appl. Phys. Lett.* **78**, 1149 (2001); D. H. Reneker, A. L. Yarin, H. Fong, and S. Koombhongse, *J. Appl. Phys.* **87**, 4531 (2000).
- [12] M. M. Hohman, M. Shin, G. C. Rutledge, and M. P. Brenner, *Phys. Fluids* **13**, 2201 (2001).
- [13] M. M. Hohman, M. Shin, G. C. Rutledge, and M. P. Brenner, *Phys. Fluids* **13**, 2221 (2001).
- [14] The electrospinning apparatus consists of two aluminum disks 10 cm in diameter at a separation up to 30 cm (Fig. 1). Fluid is delivered to the capillary via a Teflon® feedline from a syringe pump (Harvard Apparatus PHD 2000). A power supply (Gamma High Voltage Research ES-30P) provides up to 30 kV to the upper disk. Current is measured by a digital multimeter (Fluke 85 III) as the voltage drop across a 1.0 MΩ resistor between the lower disk and ground. All chemicals were purchased from Aldrich. PCL (Mw 80 000) was dissolved in a mixture of chloroform and methanol (3 to 1 by volume). The surface tensions (γ) varied between 25.0 and 28.1 dyn/cm, for the 8% and 12% solutions, respectively. The conductivity (K) of PCL solutions was 0.5 to 0.6 $\mu\text{S}/\text{cm}$. A 2 wt% solution of polyethylene oxide (PEO) (Mw 2 000 000) in water had $\gamma = 61.8$ dyn/cm and $K = 81.3$ $\mu\text{S}/\text{cm}$. Solutions of 10 and 8 wt% polyacrylonitrile (PAN) (Mw 150 000) in *N,N*-dimethyl formamide had $\gamma = 37$ dyn/cm and conductivities of 42.5 and 38.5 $\mu\text{S}/\text{cm}$, respectively. Surface tension was measured on a tensiometer (Kruss-10), conductivity was measured by a conductivity meter (Cole-Parmer-19820). Scanning electron microscopy (JOEL SEM 6320) was used to measure the fiber diameters after coating with a layer (150 Å thick) of Au/Pd.
- [15] We use $\chi = 100$ in all calculations. Values ranging from $\chi = 10$ (cf. Fig. 18 of Ref. [12]) to $\chi = 1000$ (based on $h = 100$ μm for the fluid jet at the onset of instability and $R = 10$ cm) are probably reasonable. The exact value is not critical, since $\ln \chi$ varies slowly.